XLVI CILAMCE
VITÓRIA - ES - BRAZIL - 2025
XLVI IBERO-LATIN AMERICAN CONGRESS ON COMPUTATIONAL METHODS IN ENGENEERING

Stability Analysis of Slopes subjected to rapid water level drawdown considering analytical solutions to the seepage problem

Mário V. Ceron[1], Diogo L. Cecílio[1], Renato V. Linn[1], Samir Maghous[1]

[1]*Graduate Program in Civil Engineering PPGEC/UFRGS,*
Av. Osvaldo Aranha, 99, Porto Alegre, 90035-190, RS, Brazil
mario.ceron@ufrgs.br, cecilio.diogo@gmail.com, renatolinn@ufrgs.br, samir.maghous@ufrgs.br

Abstract. The stability analysis of a saturated soil slope subjected to seepage flow generated by rapid water level drawdown is investigated in this study by means of the limit analysis kinematic approach. Adopting the framework of effective stresses for formulating the strength failure condition of the saturated porous medium, it is shown that the effect of seepage flow can be accounted for in the stability analysis by means of driving body forces computed from the gradient of pore pressure distribution. The hydraulic boundary value problem governing the water filtration velocity is addressed by resorting to a specific analytical variational approach. Comparisons with traditional pore pressure coefficient methods and finite element analyses demonstrate the effectiveness of the proposed methodology. Numerical analyses are conducted to explore the influence of hydraulic-related parameters, highlighting in particular the critical effects of water drawdown height and soil permeability anisotropy.

Keywords: Kinematic approach, Slope stability, Seepage forces, Limit analysis

1 Introduction

Stability analysis of slopes is a fundamental problem in soil mechanics. Its main objective is to evaluate the potential failure of the structure under prescribed loading conditions based solely on the strength properties of its constituent material. Water saturating the soil is known to generally reduce its shear strength. In non-hydrostatic conditions, seepage-induced effects can endanger the safety of previously stable structures, especially in rapid drawdown situations, posing a significant risk to riverside, coastal, and near dam slopes [1–3].

In a partially coupled analysis, classically referred to as one-way coupling approach, the hydraulic problem consisting of evaluating the water filtration velocity in slow and rapid drawdown conditions may be assessed independently of skeleton deformation, being subsequently incorporated as external body forces in effective stress analysis [4, 5]. This approach is widely accepted in the scientific community in kinematic approaches of limit analysis [3–8]. The above-mentioned contributions, however, employ mostly empirical methods based on pore pressure coefficients to account for the seepage influence.

In the present research, the validity of the effective stress concept is assumed for the strength capacities of saturated porous media. Following the procedure described by Saada et al. [5], the water flow regime is determined independently by resorting to a specific analytical variational approach. The resulting seepage forces, computed from the gradient of the pore pressure distribution, are regarded as driving body forces in the stability problem. Once the seepage forces are evaluated, the stability analysis is therefore developed within the framework of the limit analysis kinematic approach. The latter relies upon the implementation of rotational failure mechanisms involving velocity discontinuity along logarithmic spiral curves. Comparisons with traditional pore pressure coefficient methods and finite element analyses demonstrated the effectiveness of the proposed methodology. Numerical analyses are conducted to explore the influence of hydraulic-related parameters, highlighting in particular the critical effects of water drawdown height and soil permeability anisotropy.

2 Effective stress stability analysis

This section describes a poromechanical framework for the effective stress stability analysis of geotechnical structures in the presence of seepage forces. Along the subsequent analysis, the domain occupied by the soil material shall be referred to as Ω and its external boundary as $\partial\Omega$.

2.1 Limit Analysis of saturated slopes under plane strain condition

The primary objective of limit analysis theory and related kinematic approach is to evaluate the stability conditions of a material system under the applied loading. The plane strain stability analysis under consideration refers to a soil slope with height H and inclination β, as depicted in Figure 1. In the context of effective stress analysis, the strength capacities of the soil will be described by means of an isotropic frictional-cohesive condition governing the Terzaghi effective stress. The strength parameters of the Mohr-Coulomb criterion c and φ denote respectively the soil cohesion (effective cohesion intercept) and friction angle fields.

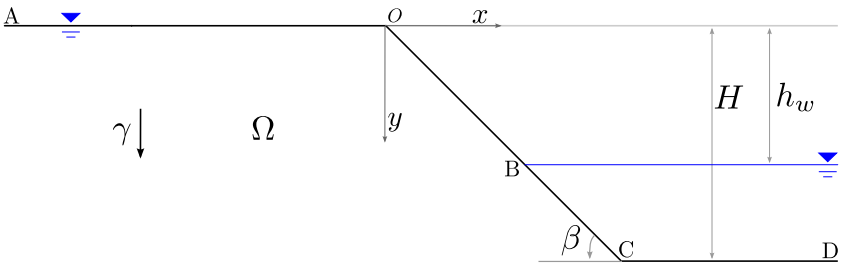


Figure 1. Slope geometry and loading configuration.

As regards the loading conditions, the slope structure is subjected to two forces: the mechanical components, which are defined by the gravity forces (saturated unit weight γ parallel to Oy direction) and boundary conditions; and the hydraulic component, originated from the pore fluid pressure p distribution associated with the flow through the slope that is induced by water drawdown (rapid decrease h_w in water level). The spatial variation of excess pore pressure distribution u, which is related to its gradient field $-\text{grad}\ u$, is expected to be the driving force for the seepage loading component. The excess pore pressure $u = p - p_w$ is defined relative to the hydrostatic pore pressure $p_w = y\gamma_w$, where γ_w denotes the water unit weight.

The kinematic approach is formulated within the framework of effective stress analysis. Denoting by $\underline{U}$ any given kinematically admissible velocity field (referred to as failure mechanism), the upper-bound theorem of limit analysis states the following necessary condition for the stability of the slope structure under applied external loading [9]:

$$\forall \underline{U} \quad P_{ext}(\underline{U}) \leq P_{mr}(\underline{U}) \tag{1}$$

where P_{ext} stands for the rate of external work performed by the external forces and P_{mr} stands for the maximum rate of resisting work developed in the failure mechanism $\underline{U}$.

In this research, the set of possible velocity fields is restricted to the class of rotational failure mechanisms involving velocity discontinuity along logarithmic spiral curves [10]. In this context, P_{ext} and P_{mr} are given by:

$$P_{ext}(\underline{U}) = \int_{\Omega} (\gamma - \gamma_w)\underline{e}_y \cdot \underline{U}\, d\Omega + \int_{\Omega} -\text{grad}\ u \cdot \underline{U}\, d\Omega, \quad P_{mr}(\underline{U}) = \int_{\Sigma} \frac{c}{\tan\varphi}[\underline{U}] \cdot \underline{n}\, dS \tag{2}$$

where $[\underline{U}]$ denotes the velocity jump at a point $\underline{x}$ when crossing a velocity discontinuity surface Σ following its normal unit vector $\underline{n}$. In the spirit of the kinematic approach, the optimal upper-bound estimate to the stability problem, denoted by the stability factor Γ, is achieved by means of the minimization of:

$$\Gamma \leq \min_{\underline{U} \in \zeta} \frac{P_{mr}(\underline{U})}{P_{ext}(\underline{U})}, \quad \text{where } P_{ext}(\underline{U}) > 0 \tag{3}$$

where ζ symbolically represents the class of admissible rotational failure mechanisms considered. Values of Γ lower than unity mean necessary failure of the slope.

3 The hydraulic problem

Traditionally, the seepage influence on the stability of saturated slopes is accounted for by employing empirical methods based on pore pressure coefficients. The major drawback of such an approach is that the value of the coefficients to be used for a given stability configuration is a priori unknown. In the present study, the alternative approach described by Saada et al. [5] is considered. As stated in the effective stress formulation of the slope stability problem presented in the previous section, the effects of seepage forces may be accounted for through the distribution of $-\text{grad}\ u$ (Eq. 2), which act as external body forces that should therefore be previously evaluated.

In that respect, the gradient of excess pore pressure is the driving force of the hydraulic flow network through the slope and is classically related to the filtration velocity field $\underline{v}$ by Darcy's law:

$$\underline{v} = -\underline{\underline{K}} \cdot \text{grad}\, u \tag{4}$$

where $\underline{\underline{K}}$ denotes the fluid permeability tensor expressed in $\text{m}^2 \cdot \text{Pa}^{-1} \cdot \text{s}^{-1}$ unit. Introducing the vertical k_v and horizontal k_h permeability coefficients, with $k_h \geq k_v$, the permeability tensor is assumed throughout the study to take the following form:

$$\underline{\underline{K}} = k_h \underline{e}_x + k_v \underline{e}_y \tag{5}$$

The permeability anisotropy is thus characterized by the value of the ratio $\alpha = k_h/k_v \geq 1$.

Under the assumptions of steady flow, incompressibility of the solid as well as fluid particles, and neglecting the skeleton volume strain (one-way coupling framework), the field equation controlling the uncoupled hydraulic problem is given by:

$$\text{div}\, \underline{v} = 0 \tag{6}$$

The formulation of the uncoupled hydraulic boundary value problem in terms of the excess pore pressure u relies on the field equation (6) and Darcy's law (4), together with the prescribed hydraulic boundary conditions. The pore water pressure is set to $p = 0$ along the surfaces $\overline{AO}$ and $\overline{OB}$ (see Figure 1), and to $p = (y - h_w)\gamma_w$ along $\overline{BC}$ and $\overline{CD}$, corresponding to the hydrostatic distribution on the external boundary. Expressed in terms of the excess pore pressure $u = p - y\gamma_w$, the boundary value problem becomes

$$\begin{cases} \text{div}\, (-\underline{\underline{K}} \cdot \text{grad}\, u) = 0 & \text{in } \Omega, \\ u = 0, & \text{on } \overline{AO} \\ u = -y\gamma_w, & \text{on } \overline{OB}, \\ u = -h_w\gamma_w, & \text{on } \overline{BC} \cup \overline{CD} \end{cases} \tag{7}$$

3.1 Variational formulations for the uncoupled hydraulic problem

The uncoupled hydraulic boundary value problem consists of finding the excess pore pressure field u solution to problem (7). The latter is a classical elliptic differential problem, which is usually addressed numerically by the finite element method. This approach is based on the well-known variational theorem stating that the solution u achieves the minimum of the following hydraulic functional (homogeneous to an energy rate):

$$J(u') = \frac{1}{2} \int_\Omega \text{grad}\, u' \cdot \underline{\underline{K}} \cdot \text{grad}\, u'\, d\Omega + \int_{\partial\Omega_v} u' v^d\, dS \tag{8}$$

over the set $\mathcal{P}$ of admissible pore pressure distributions u', that is

$$u' \in \mathcal{P} \iff u' \text{ is continuous and piecewise differentiable, and } u' = u^d \text{ on } \partial\Omega_u \tag{9}$$

where $\partial\Omega_u$ and $\partial\Omega_v$ denote, respectively, the boundaries of the domain with prescribed excess pore pressure and filtration velocity. For context, $\partial\Omega_u = \overline{AO} \cup \overline{OB} \cup \overline{BC} \cup \overline{CD}$ and $\partial\Omega_v = \emptyset$ for the problem stated in (7).

Keeping in mind that the seepage forces are defined in the stability problem by the gradient of excess pore pressure, it would be more appropriate to formulate a variational approach of the boundary value problem (7) in terms of velocity filtration $\underline{v}$ related to $\text{grad}\, u$ through (4). In that respect, and following the approach developed de Buhan et al. [11], it is shown that the solution $\underline{v}$ in terms of velocity filtration of the differential problem (7) achieves the minimum of the following hydraulic functional (also homogeneous to an energy rate):

$$J^*(\underline{v}') = \frac{1}{2} \int_\Omega \underline{v}' \cdot \underline{\underline{K}}^{-1} \cdot \underline{v}'\, d\Omega + \int_{\partial\Omega_u} u^d \underline{v}' \cdot \underline{n}\, dS \tag{10}$$

over the set $\mathcal{V}$ of admissible filtration velocity distributions $\underline{v}'$, that is

$$\underline{v}' \in \mathcal{V} \iff \begin{cases} \underline{v}' \text{ is piecewise continuous and differentiable} \\ \text{the normal component } \underline{v}' \cdot \underline{n} \text{ remains continuous across discontinuity surfaces } \Sigma \text{ of } \underline{v}' \\ \text{div}\, \underline{v}' = 0 \text{ in } \Omega \text{ and } \underline{v}' \cdot \underline{n} = v^d \text{ on } \partial\Omega_v \end{cases} \tag{11}$$

The conjunction of the two minimum principles expresses the upper and lower boundaries to the energy of the hydraulic problem, as summarized in the following equation:

$$\forall u' \in \mathcal{P},\ \forall \underline{v}' \in \mathcal{V} \quad -J(u') \leq -J(u) = J^*(\underline{v}) \leq J^*(\underline{v}') \tag{12}$$

where u and $\underline{v}$ denote the solutions to the differential problem (7).

3.2 Solutions to the uncoupled hydraulic problem

Based on the implementation of the variational principle of minimum in filtration velocity, the approach consists in considering a class of admissible filtration velocity fields $\underline{v}'$ and then determining the best approximation within the considered class by a minimization procedure of the functional $J^*(\underline{v}')$. Referring to the polar coordinates $(O,\ r,\ \theta)$ and notations defined in Figure 2, the general expression of filtration velocity fields is given for any point $\underline{x}$ of coordinates $(r,\ \theta)$ by the following equations:

$$\underline{v}'(\underline{x}) = \begin{cases} \underline{v}_1 = -h_1(r)\dfrac{d}{d\theta}h_2(\theta)\ \underline{e}_r + \dfrac{d}{dr}(r\ h_1(r))h_2(\theta)\ \underline{e}_\theta & \text{for } 0 \le r < R_w \\ \underline{v}_2 = h_3(r)\ \underline{e}_\theta & \text{for } R_w \le r < R \\ \underline{v}_3 = h_4(r)\ \underline{e}_\theta & \text{for } R \le r < R_e \\ 0 & \text{for } r \ge R_e \end{cases} \tag{13}$$

where $\underline{e}_\theta$ represents the unit orthoradial vector, $R_w = h_w/\sin\beta$, $R = H/\sin\beta$, and R_e is a geometrical parameter defining the external radius of the flow zone. Functions $r \to h_i(r)$ for $i \in \{1,\ 3,\ 4\}$ and $\theta \to h_2(\theta)$ are assumed to be continuously differentiable with imposed condition $h_1(R_w) = 0$. It can readily be shown that $\underline{v}' \in \mathcal{V}$. Figure 2 presents the domain definition and polar system considered.

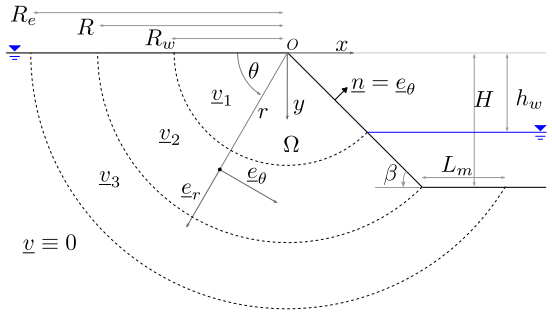


Figure 2. Description of the geometrical zones involved in the definition of piecewise filtration velocity field.

The best approximation $\underline{v}' = \underline{v}'_{opt}$ within the considered class of filtration velocity fields is obtained from stationary conditions of functional $J^*(\underline{v}')$ with respect to functions h_i. After some mathematical development, the optimal field solution $\underline{v}'_{opt}$ is defined by the following local fields $\underline{v}_i$:

$$\underline{v}_1 = \frac{k_h h_2(\pi-\beta)\gamma_w \sin\beta}{C-D}\left[\left(1 - \frac{C}{D}\left(\frac{r}{R_w}\right)^{\frac{C}{D}-1}\right) h_2(\theta)\ \underline{e}_\theta - \left(1 - \left(\frac{r}{R_w}\right)^{\sqrt{\frac{C}{D}}-1}\right)\frac{d}{d\theta}h_2(\theta)\ \underline{e}_r\right] \tag{14}$$

$$\underline{v}_2 = \frac{k_h\gamma_w h_w}{(\alpha+1)\dfrac{\pi-\beta}{2} - (\alpha-1)\dfrac{\sin 2\beta}{4}}\ \frac{1}{r}\ \underline{e}_\theta;\ \underline{v}_3 = \frac{2k_h\gamma_w h_w}{(\alpha+1)\left[\pi - \arcsin\frac{H}{r}\right] - (\alpha-1)\dfrac{H\sqrt{r^2-H^2}}{r^2}}\ \frac{1}{r}\ \underline{e}_\theta \tag{15}$$

Parameters C and D are defined by the following integrals:

$$C = \int_0^{\pi-\beta}\left(\frac{d}{d\theta}h_2(\theta)\right)^2(\cos^2\theta + \alpha\sin^2\theta)\ d\theta; \quad D = \int_0^{\pi-\beta}(h_2(\theta))^2(\sin^2\theta + \alpha\cos^2\theta)\ d\theta \tag{16}$$

Function $h_2(\theta)$ is solution to the second-order ordinary differential equation:

$$h_2''(\theta) + \frac{(\alpha-1)\sin 2\theta}{\cos^2\theta + \alpha\sin^2\theta}h_2'(\theta) - \sqrt{\frac{C}{D}}\frac{\sin^2\theta + \alpha\cos^2\theta}{\cos^2\theta + \alpha\sin^2\theta}h_2(\theta) = 0 \tag{17}$$

In addition, function $h_2(\theta)$ is subjected to the following conditions:

$$h_2'(0) = 0; \quad h_2'(\pi-\beta) = \frac{2\sqrt{C}\left(\sqrt{C}+\sqrt{D}\right)}{R_w^2(\cos^2\beta + \alpha\sin^2\beta)}\frac{(D-C)^2}{(\sqrt{C}-\sqrt{D})^2}\frac{1}{h_2(\pi-\beta)k_h\gamma_w\sin\beta} \tag{18}$$

Since the coefficients C and D in the above differential equation are explicitly depending on function $h_2(\theta)$ through (16), the solution function $h_2(\theta)$ to (17) is evaluated numerically using LSODA solver in Python-based framework [12]. Once the optimal filtration velocity field is determined, the seepage forces required for the next step of the slope stability are approximated by $-\text{grad}\ u \approx \underline{\underline{K}}^{-1} \cdot \underline{v}'_{opt}$. Additional details are provided in Ceron et al. [13].

3.3 Comparison of Semi-Analytical and Finite Element Approaches to the Hydraulic Problem

To assess the accuracy of the above semi-analytical solution to the hydraulic problem based on the variational principle in filtration velocity, a standard finite element analysis implementing the classical variational theorem of minimum in pore pressure (minimization of functional $J(u')$ given by (8)) has been performed. Six-noded triangular elements were employed to obtain approximations u'_{FE} to the excess pore pressure distribution. It should be noted, however, that u'_{FE} does not generally satisfy the continuity condition of the gradient $\mathrm{grad}\, u'_{FE}$ between adjacent elements.

The two variational formulations presented cannot be directly compared in terms of their solutions. One yields a semi-analytical approximation of the velocity field, while the other provides a finite element approximation of the excess pore pressure distribution. Their comparison is meaningful only through the associated hydraulic functional values. The conjunction of the two variational principles described in (12) indicates that the functional calculated for the solution to the original hydraulic problem (7) is bracketed by $J^*(\underline{v}'_{opt})$ (semi-analytical velocity solution) and $J(u'_{FE})$ (finite element pore pressure solution). Figure 3 depicts the variations of these two quantities, normalized by $k_h H^2 \gamma_w^2$, as functions of the slope inclination β. Several values of the permeability anisotropy ratio $\alpha = k_h/k_v \geq 1$ have been considered.

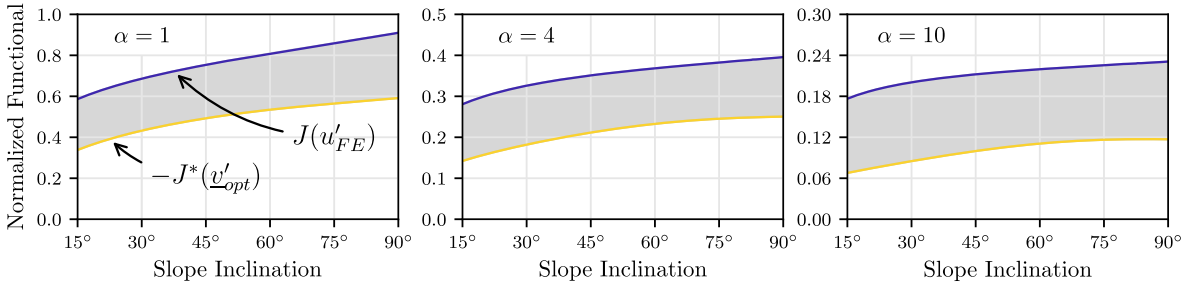


Figure 3. Comparison of hydraulic functional estimates obtained from the two variational approaches.

In this representation, the yellow curve indicates the semi-analytical optimal solution, and the blue curve corresponds to the finite element solution. The gray band represents the region within which the functional curve of the exact solution to the hydraulic problem (7) must lie. It should be noted that this representation does not indicate which of the two approaches provides a closer approximation to the exact solution.

To conclude with the hydraulic problem and before moving to numerical applications, some comments regarding the empirical concept of pore pressure coefficient deserve to be stated at this stage. The latter concept, commonly used to evaluate the effects of pore water pressure in slope stability analyses, is based on the approximate framework originally proposed by Bishop and Morgenstern [14]: $r_p = p/(\gamma h)$, where h stands for the vertical depth of the point located on the failure surface below the soil surface.

Since it explicitly depends on the pore pressure distribution p, coefficient r_p is naturally expected to vary spatially within the slope soil mass. However, most slope stability approaches using this concept to evaluate pore water pressure effects operate with a constant average value of r_p throughout the entire cross-section considered by the slope failure mechanism. Values below 0.3 are generally adopted for the pore pressure coefficient in these analyses. The major drawback of such a simplified approach lies in the fact that the value of r_p to be used for a given stability configuration is a priori unknown.

4 Numerical Aplications

This section provides preliminary numerical results derived from implementation of the kinematic approach formulated within the context of effective stress concept. The first application refers to the slope stability analysis under rapid water level drawdown addressed in Wu et al. [3], while the second illustrative application aims at assessing the effects of permeability analysis on the stability factor.

4.1 Comparison with stability analysis based on pore pressure coefficient Wu et al. [3]

The predictions derived from the present approach are compared to the upper bound solutions obtained in Wu et al. [3] for the stability condition of coastal clay slopes subjected to sea level rapid drawdown. In the latter analysis, the authors considered a constant pore pressure coefficient r_p to evaluate the effects of seepage forces. The study refers to two slopes configurations, respectively in Israeli clay ($c = 6$ kPa, $\varphi = 32°$) and London clay ($c = 11.7$ kPa, $\varphi = 24.7°$), both with a a soil unit weight of $\gamma = 18$ kPa.

It is observed that a specific aspect of the comparative study is to assess the impact of using different approaches to evaluate the pore water pressure effects in the slope stability analysis. In that respect, the seepage forces considered in the rotational failure mechanisms are computed either from the semi-analytical variational principle in filtration velocity (i.e., $-\text{grad}\, u \approx \underline{\underline{K}}^{-1} \cdot \underline{v}'_{opt}$) or from finite element approach to hydraulic problem (i.e., $-\text{grad}\, u'_{FE}$). Figure 4 presents the plots of critical height estimate for Israeli clay slope and London clay slope as a function of water drawdown ratio h_w/H, considering in each configuration two typical values of the slope inclination. A homogeneous isotropic permeability ($\alpha = k_h/k_v = 1$) has been considered in the hydraulic problem. Although the three approaches provide ample evidence of the destabilizing effects that are induced by increasing water drawdown height they showed substantial gaps in terms of critical height prediction (up to 40% in the case of the London clay slope).

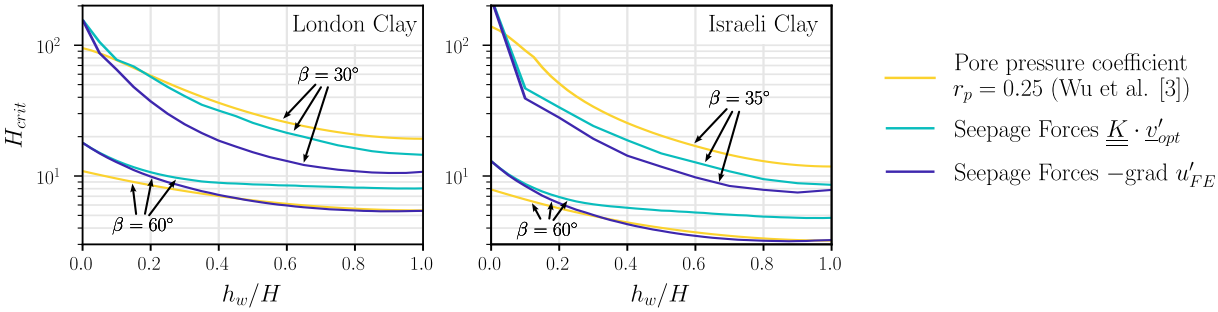


Figure 4. Slope critical height predictions associated with three distinct approaches to the hydraulic problem.

The major drawback of operating with an average r_p is that such a value is a priori unknown, introducing an uncontrolled approximation that cannot be interpreted as underestimating or as overestimating the effect of pore pressure. On the other hand, the approach based on variational principle in filtration velocity $-\text{grad}\, u \approx \underline{\underline{K}}^{-1} \cdot \underline{v}'_{opt}$ as well the finite element approach based on the variational principle in pore pressure $-\text{grad}\, u'_{FE}$ represent upper and lower estimates of seepage forces in the variational sense described by inequalities (12).

4.2 Effects of permeability anisotropy on slope stability

Restricting the study to a particular configuration of slope geometry, soil strength properties and loading conditions, the objective herein is to provide preliminary insight into the effects of soil permeability anisotropy on the slope stability factor. Numerical evaluations of the stability factor have been performed considering the following set of data: slope heigh $H = 5$ m, slope inclination β ranging from $15°$ to $90°$, soil cohesion and friction angle ($c = 10$ kPa, $\varphi = 30°$), soil unit weight $\gamma = 20$ kN/m^3, total water level drawdown $h_w = H$. Anisotropy of the soil permeability is reflected by the value of ratio $\alpha = k_h/k_v$, which is taken equal to 1 (isotropy), 5 and 10. For each selected model data, the numerical value of the upper bound estimates for Γ has been obtained from the class of rotational failure mechanisms considering either the approximation $-\text{grad}\, u \approx \underline{\underline{K}}^{-1} \cdot \underline{v}'_{opt}$ or $-\text{grad}\, u'_{FE}$ for seepage forces. Figure 5 presents the variations of stability factor Γ as a function of slope inclination β.

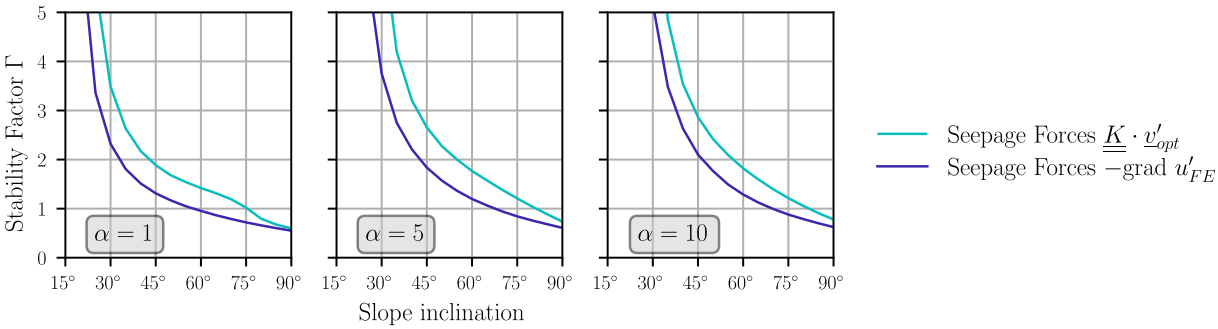


Figure 5. Effect of the anisotropy coefficient on the stability factor.

It was observed from these results that both approaches used for evaluating the seepage forces suggest that higher values of the permeability anisotropy ratio α lead to higher stability factors for all slope inclinations, predicting an increase in slope stability. Such a trend is consistent with the results observed, for instance, in the context of face stability analysis of shallow tunnels driven under the water table [11], which indicate that a higher α has a favorable effect on tunnel face stability.

5 Conclusions

In this research, the limit analysis kinematic approach formulated within the effective stress context has been applied to address the stability problem of slopes subjected to rapid water level drawdown. Particular emphasis is devoted to the evaluation of seepage forces induced in the slope by water drawdown and derived from the gradient of excess pore pressure distribution. The latter can be obtained from the solution to an uncoupled hydraulic boundary value problem, for which a variational formulation in terms of filtration velocity is presented. Rigorous upper-bound solutions for the slope stability factor can therefore be derived from the implementation of the kinematic approach by means of the class of rotational log-spiral failure mechanisms.

The accuracy of the approach has been assessed by comparison with available results based on the concept of pore pressure coefficient. Numerical analyses have been presented with the objective of providing preliminary insight regarding the influence of relevant problem parameters. The results have particularly emphasized the destabilizing effects of seepage forces reflected by a significant reduction in the slope stability factor associated with increasing water drawdown ratio. Investigation of the role of the soil permeability anisotropy has clearly indicated that a higher horizontal permeability as compared with the vertical one has a favorable effect on the slope stability.

Acknowledgements. The authors gratefully appreciate the support provided by the Brazilian Research Council (CNPq) and the Brazilian Federal Agency for Support and Evaluation of Graduate Education (CAPES).

Authorship statement. The authors hereby confirm that they are the sole liable persons responsible for the authorship of this work, and that all material that has been herein included as part of the present paper is either the property (and authorship) of the authors, or has the permission of the owners to be included here.

References

[1] N. Moregenstern. Stability charts for earth slopes during rapid drawdown. *Géotechnique*, vol. 13, n. 2, pp. 121–131, 1963.
[2] J. M. Duncan, S. G. Wright, and K. S. Wong. Slope stability during rapid drawdown. In *Proceedings of the H. Bolton Seed Memorial Symposium*, volume 2, pp. 253–272, 1990.
[3] D. Wu, X. Chen, and J. Zhang. Effect of sea level drawdown on coastal clay slope stability considering two strength criteria. *Marine Georesources & Geotechnology*, vol. , pp. 1–19, 2024.
[4] C. Viratjandr and R. L. Michalowski. Limit analysis of submerged slopes subjected to water drawdown. *Canadian Geotechnical Journal*, vol. 43, n. 8, pp. 802–814, 2006.
[5] Z. Saada, S. Maghous, and D. Garnier. Stability analysis of rock slopes subjected to seepage forces using the modified hoek–brown criterion. *International Journal of Rock Mechanics and Mining Sciences*, vol. 55, pp. 45–54, 2012.
[6] R. L. Michalowski and S. S. Nadukuru. Three-dimensional limit analysis of slopes with pore pressure. *Journal of Geotechnical and Geoenvironmental Engineering*, vol. 139, n. 9, pp. 1604–1610, 2013.
[7] Y. Gao, D. Zhu, F. Zhang, G. Lei, and H. Qin. Stability analysis of three-dimensional slopes under water drawdown conditions. *Canadian Geotechnical Journal*, vol. 51, n. 11, pp. 1355–1364, 2014.
[8] Q. Pan, J. Xu, and D. Dias. Three-dimensional stability of a slope subjected to seepage forces. *International Journal of Geomechanics*, vol. 17, n. 8, pp. 04017035, 2017.
[9] J. Salençon. *Yield Design*. Mechanical engineering and solid mechanics series. ISTE Ltd and John Wiley & Sons, London, England, 2013.
[10] W.-F. Chen. *Limit Analysis and Soil Plasticity*. Elsevier, 1975.
[11] de P. Buhan, A. Cuvillier, L. Dormieux, and S. Maghous. Face stability of shallow circular tunnels driven under the water table: a numerical analysis. *International Journal for Numerical and Analytical Methods in Geomechanics*, vol. 23, n. 1, pp. 79–95, 1999.
[12] L. Petzold. Automatic selection of methods for solving stiff and nonstiff systems of ordinary differential equations. *SIAM Journal on Scientific and Statistical Computing*, vol. 4, n. 1, pp. 136–148, 1983.
[13] M. V. Ceron, D. L. Cecílio, R. V. Linn, and S. Maghous. Stability analysis of slope subjected to seepage forces considering spatial variability of soil properties. *International Journal for Numerical and Analytical Methods in Geomechanics*, vol. 49, n. 11, pp. 2459–2491, 2025.
[14] A. W. Bishop and N. Morgenstern. Stability coefficients for earth slopes. *Géotechnique*, vol. 10, n. 4, pp. 129–153, 1960.